ACS OMEGA

http://pubs.acs.org/journal/acsodf

Article

Fabrication of Zwitterion TiO_2 Nanomaterial-Based Nanocomposite Membranes for Improved Antifouling and Antibacterial Properties and Hemocompatibility and Reduced Cytotoxicity

Kanagaraj Venkatesh, G. Arthanareeswaran,* Palaniswamy Suresh Kumar, and Jihyang Kweon

Cite This: *ACS Omega* 2021, 6, 20279−20291

Read Online

ACCESS | Metrics & More | Article Recommendations | Supporting Information

ABSTRACT: Although zwitterion nanomaterials exhibit outstanding antifouling property, hemocompatibility, and antibacterial activity, their poor solubility in organic solvents limits their practical applications. In the present study, natural lysine (amino acids) was surface-grafted onto one-dimensional (1D) TiO_2 nanofibers (NFs) through an epoxy ring opening in which the 3-glycidyloxypropyl (dimethoxy) methyl silane was used as a coupling agent. Chemical binding and morphological studies, such as Fourier transform infrared spectroscopy, X-ray photoelectron spectroscopy, and transmission electron microscopy, were conducted to confirm the successful grafting of lysine onto the TiO_2 NFs. The lysine-grafted TiO_2 NF-polyethersulfone (PES) membrane induced electrostatic interactions and increased the surface charges from −28 to 16 mV in ζ-potential analysis. The lysine exhibited zwitterion characteristics owing to the presence of amino (cations) and carboxyl (anions) functional groups. Moreover, the modified TiO_2-PES zwitterion membranes exhibited good water flux performances compared to the pristine membrane. ZT-4 membrane displayed the highest water fluxand bovine serum albumin (BSA) rejection of 137 ± 1.8 L m^{-2} h^{-1} and 94 ± 1%, respectively. The cell viability results revealed that the zwitterion PES membrane had excellent biocompatibility with peripheral blood mononuclear cells. The present work offers a convenient strategy to improve the hydrophilicity, antifouling property, and hemocompatibility of modified TiO_2-PES zwitterion membranes for their biomedical and blood-contacting applications such as hemodialysis.

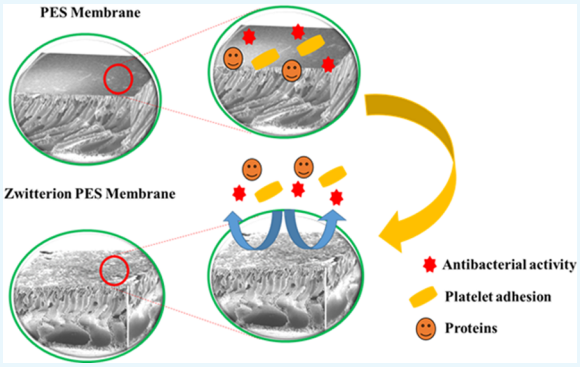

1. INTRODUCTION

Globally, many patients suffer from end-stage renal disease. Of late, artificial membranes have caught the attention of various researchers as some of these membranes are being commercially employed for water filtration and biomedical applications.[1−3] However, there are several problems associated with the synthesis of artificial membranes for biomedical applications, such as (1) nonspecific proteins that affect the water flux and membrane lifetime; (2) thrombus formation and blood component initiation;[4] (3) bacterial infections, which affect the membrane matrix owing to the establishment of bacterial biofilms;[5] and (4) cytotoxicity, where foreign materials are in contact with the blood, resulting in harmful effects.[6] To address all of these issues, researchers have adopted several modified approaches to enhance the antifouling, hemocompatibility, and antibacterial activity by minimizing the cytotoxicity.

A few methods, such as physical blending, chemical grafting, surface plasma treatment, and layer-by-layer (LbL) assembly, have been adopted to design specific functional biointerfaces.[7] Among these methods, surface grafting is a promising technique that endows materials with specific biofunctionality and biocompatibility. However, surface chemical grafting requires complex physical/chemical treatments to achieve active chemical groups. Therefore, it is crucial to devise new approaches to develop inexpensive, effective, and stable surface grafting methods for the design of bioactive material interfaces. Recent advanced developments in chemistry and material science have resulted in several artificial polymers for use in hemodialysis.[8−10] Polyethersulfone (PES) is a promising membrane material because of its superior chemical, thermal, and hydrolytic stability, together with better mechanical and membrane formation.[2] However, the hydrophobic properties of PES and membrane fouling are prevalent, leading to flux drop during real feed operation.[11] Moreover, when PES is employed as a hemodialysis membrane, it can affect protein adsorption, thrombus formation, platelet adhesion, and bacterial infections, which may be harmful to patients.[12]

Received: April 23, 2021
Accepted: July 13, 2021
Published: July 27, 2021

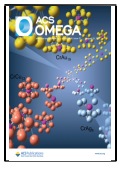

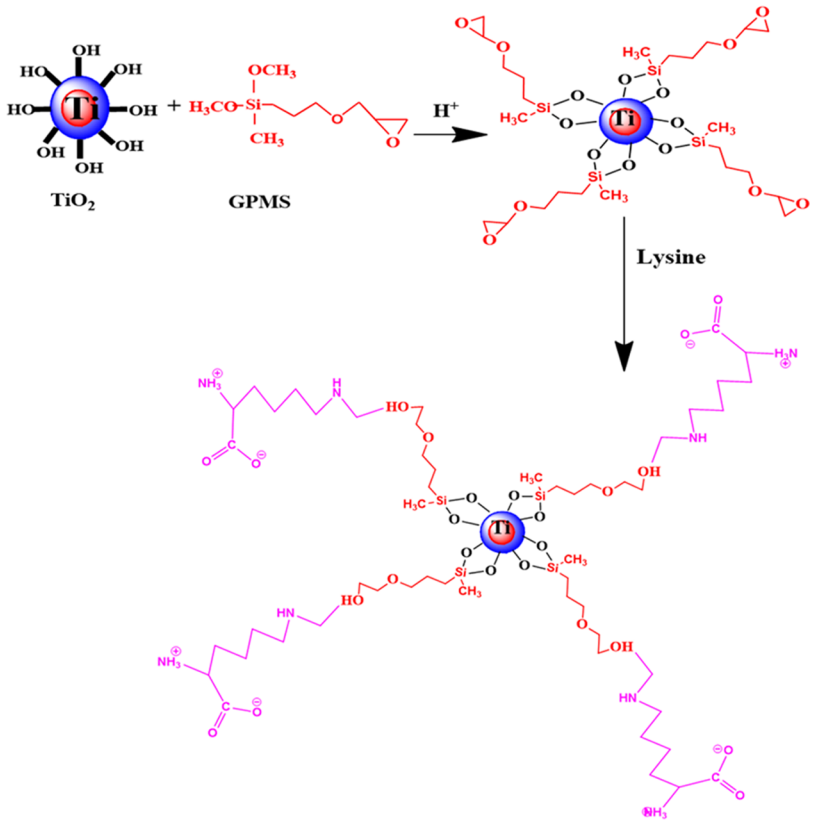

Figure 1. Schematic illustration of the fabrication of a zwitterion TiO_2 NF.

To resolve the abovementioned complications through the application of modified PES membranes for hemodialysis, several methods have been used to improve the antifouling and bactericidal activities and hemocompatibility with reduced cytotoxicity.[13−15] Poly(ethylene glycol) (PEG) and polyglycol (PG) are widely used in earlier research studies as benchmark biocompatible and antifouling modifiers in medical applications,[16−20] It is believed that PEG and PG chains could not provide steric repulsion to the approaching biomacromolecules but could bind a mass of water through hydrogen bonding, generating a "barrier" to resist the adsorption/adhesion of biomacromolecules,[21−23] and thus providing excellent antibiofouling ability to the substrates. During the past two decades, zwitterion materials have attracted considerable attention and have been generally viewed as a new class of antifouling material. The unique zwitterion structures, simultaneously possessing cationic and anionic residues yet overall electrically neutral, could stabilize/maintain the native conformation of proteins[24] and inhibit nonspecific protein adsorption. Among several products of nanotechnology, TiO_2 nanofibers have shown unique combinations in terms of high specific surface area, flexibility, and porous structure.[25−27] Larger specific surface area and higher porosity contribute to an increase of hydrophilicity, water flux, antifouling, and photocatalytic reaction sites, simultaneously promoting efficiency of electron−hole pair separation. Negatively or positively charged functional groups were grafted onto nanomaterials to improve their compatibilities with the polymer matrix and, consequently, improve permeability and salt rejection. The zwitterion amino acids that lysine are popularly selected for generating low-fouling zwitterion bonds.[28] The specific combination of negative and positive charges in lysine groups in the polymer chain has shown significant resistance to fouling by bacteria, mammalian cells, human blood serum, and certain proteins.[29−31] In addition, due to the particle surface being covered with reactive active sites, TiO_2 nanoparticles are ideal carriers of functional materials, but agglomeration is a major factor limiting their application. Zwitterion nanoparticles can be prepared through surface modification, which will overcome the problems with application such as the agglomeration of nanomaterials and insolubility of zwitterion materials in organic solvents. Therefore, in this study, zwitterion TiO_2 including amine and carboxylic groups have received much greater attention for biomedical applications due to their biomimetic nature, long-term stability, excellent hydrophilicity, effectiveness in resisting nonprotein fouling, and thrombosis. It has been hypothesized that zwitterion materials with both positively and negatively charged moieties could form a hydration layer via electrostatic interaction and a hydrogen bond, leading to excellent antifouling property and biocompatibility. Despite the high density of ion pairs attached to the PES polymer chain, the overall charge of zwitterion nanomaterials is neutral under normal conditions.

In the present study, bioinspired lysine (amino acid), with 3-glycidyloxypropyl (dimethoxy) methyl silane (GPMS, KH560) as a coupling agent, was used for the uniform surface grafting of one-dimensional (1D) TiO_2 NFs containing $-NH_3^+$ and $-COO^-$ functional groups, thus exhibiting zwitterion properties. The lysine used to modify the 1D TiO_2 nanofibers (NFs) to make zwitterion brushes on the surface was prepared by blending the PES membrane with an innovative additive of zwitterion TiO_2 nanomaterials. The water permeability and the bovine serum albumin (BSA) protein antifouling property

https://doi.org/10.1021/acsomega.1c02151
ACS Omega 2021, 6, 20279−20291

Table 1. Composition, Surface Roughness, and Thermal Stability of Pristine PES and Zwitterion PES Membranes

membrane description	PES (wt %)	zwitterion TiO_2 (wt %)	NMP (wt %)	average roughness (nm)	RMS roughness (nm)	T_d (°C)	weight loss (%)
ZT-1	17.5	0	82.5	73.85	97.34	534	33
ZT-2	17.9	0.4	82.5	81.07	102.17	538	36
ZT-3	16.9	0.6	82.5	90.40	110.83	544	39
ZT-4	16.3	1.2	82.5	146.82	202.12	583	44

were studied. The blood compatibility (protein adsorption and platelet adhesion) and cytocompatibility were also investigated. This work demonstrates the importance of using a bioinspired surface-grafted zwitterion PES membrane to develop a gentle and novel strategy to improve the antifouling and antibacterial activities and hemocompatibility and reduce the cytotoxicity for biomedical applications.

2. EXPERIMENTAL SECTION

2.1. Chemicals. PES was obtained as a polymer from Sigma-Aldrich, India. Titanium butoxide (TNBT), poly(vinylpyrrolidone) (PVP), acetic acid, hydrochloric acid (HCl), and *N*-methyl-2-pyrrolidone (NMP) were purchased from Merck, India. Lysine, (3-glycidyloxypropyl) trimethoxysilane GPMS, bovine serum albumin (BSA), thiazole orange (TO), and propidium iodide (PI) were procured from Sigma-Aldrich, India.

2.2. Synthesis of Zwitterion 1D TiO_2 NFs. The electrospinning technique was adopted for the synthesis of 1D TiO_2 NFs. First, 1.5 g of TNBT was added to 10 mL of acetic acid and the mixture was stirred vigorously for 10 h. Then, 3 g of PVP polymer was mixed with the above solution. The prepared mixture was transferred to a 10 mL syringe. The distance between the syringe needle and the collector was 10 cm under an applied voltage of 18 kV and a flow rate of 1 mL h^{-1}. The resultant 1D TiO_2 NFs were collected on the collector and sintered at 250 °C for 6 h. One gram (1 g) of the as-prepared 1D TiO_2 NFs was dispersed in 40 mL of an ethanol aqueous solution under ultrasonication for 30 min to thoroughly disperse the TiO_2 nanomaterial. Then, 0.3 mL of GPMS, KH560, and 1 mL of HCl were added to the aqueous solution under magnetic stirring at 60 °C for 6 h. Thereafter, lysine (5 mL) was added to the 1D TiO_2 nanomaterial solution under magnetic stirring for 4 h. The attained product was centrifuged and dried at 60 °C for 12 h. Based on a previous work and the literature, the concentration of zwitterion TiO_2 was chosen. Figure 1 shows the zwitterion modification method of the TiO_2 nanomaterials. The coupling agent GPMS, KH560, was added to the TiO_2 nanomaterials under acidic conditions to produce the intermediate with epoxy. Through the ring-opening reaction between the NH_3 group of lysine and the epoxy groups on the TiO_2 surface, lysine with NH_3 and −COOH groups was grafted onto TiO_2 nanomaterials to obtain zwitterion nanomaterials with lysine.

2.3. Preparation of Membranes. Pristine PES and modified membranes were fabricated in a coagulation bath by the phase inversion method. Varying concentrations of zwitterion TiO_2 were added to the NMP solvent to prepare a homogenous mixture under ultrasonication treatment for 1 h. After sonication, the PES polymer was added to the above mixture under stirring for 24 h. The resultant homogenous dope solution was allowed to stand for 5 h with slow mixing. The dope solution was then spread onto a cleaned glass plate using 250 μm thin-film applicators. After 30 s of exposure, the glass plate was dipped in a coagulation bath of deionized water at room temperature for 12 h to separate the remaining solvent. The compositions of the membranes are described in Table 1.

2.4. Chemical Compositions and TEM Analysis of Zwitterion TiO_2. The surface functional groups of TiO_2, zwitterion TiO_2, and the membranes were characterized using a Shimadzu FTIR-ATIR spectrophotometer in the range of 3800−550 cm^{-1}. The surface modification of the zwitterion TiO_2 was also characterized by X-ray photoelectron spectroscopy (XPS; PHI-5000 III, FEI Inc.). Modified zwitterion TiO_2 was characterized using a transmission electron microscope (FEI Technai, F20 USA).

2.5. Membrane Characterization. The surface hydrophilicities of the membranes were evaluated using dynamic water contact angle measurements (AST Products, Inc., Billerica, MA). Membrane roughness was analyzed by atomic force microscopy (AFM) (NT-MDT modular AFM, NTEGRA Prima, Ireland). Pore-size distribution was measured using a Micromeritics Gemini V and the Brunauer−Emmett−Teller (BET) method. The thermal properties of the prepared membranes were determined using thermal gravimetric analysis (TGA, model TGA 4000, Perkin Elmer). The membrane surface charge was characterized by ζ-potentials (Surpass Anton Paar, Austria). Each sample was cut to a size of 1 × 2 cm^2, and the membrane samples were positioned in an adjustable gap cell. A sodium chloride (NaCl) solution (1 mmol L^{-1}) was used as the electrolyte to determine the ζ-potentials, which were measured at pH values of 2−10. A hydrochloric acid (HCl) solution (0.05 mol L^{-1}) and a sodium hydroxide (NaOH) solution (0.05 mol L^{-1}) were used to adjust the pH. The membrane morphologies were recorded using a JOEL JMS-6400 field emission scanning electron microscope (FESEM). The elemental mapping compositions were studied using energy-dispersive X-ray analysis.

2.6. Filtration Tests. All filtration tests were performed using a dead-end ultrafiltration module with a membrane area of 3.7 cm^2 under a membrane pressure of 2 bar. Water flux (L m^{-2} h^{-1} bar^{-1}) and BSA rejection (%) values were measured to calculate the membrane rejection performance. Flux (J) and BSA removal (R) were determined using the following respective equations

$$J = \frac{V}{A \times t} \tag{1}$$

$$R = \left(1 - \frac{C_p}{C_f}\right) \times 100\% \tag{2}$$

where A (m^2) is the effective area, V (L) is the volume, and t (h) is the collecting time. C_f and C_p are the initial and final BSA concentrations, respectively.

2.7. Antifouling Studies and Leaching Tests. Protein antifouling is an important factor for blood-contacting materials in the design of hemocompatibility studies. To study the antifouling performance, the following steps were conducted using dead-end ultrafiltration (UF Model cell

https://doi.org/10.1021/acsomega.1c02151
ACS Omega 2021, 6, 20279−20291

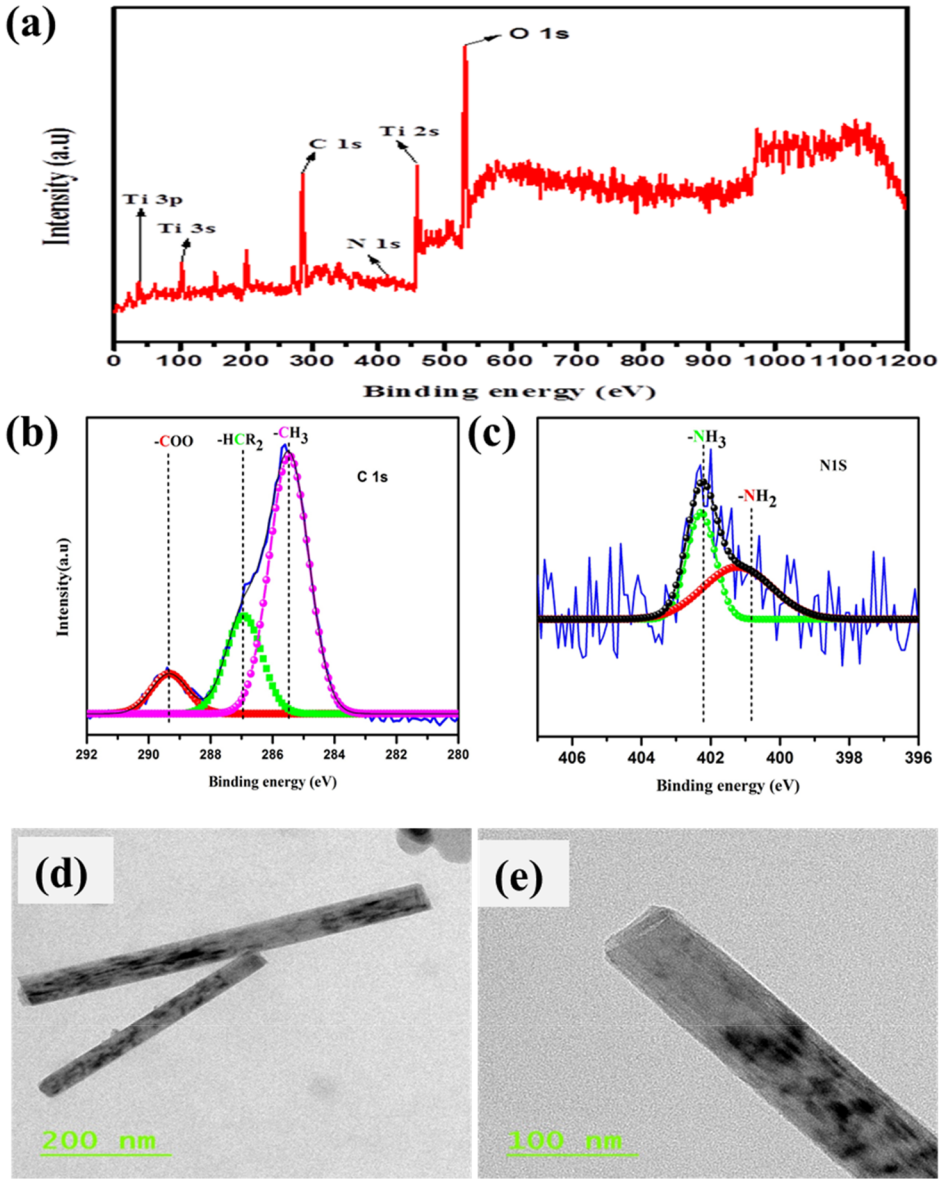

Figure 2. XPS spectroscopy for zwitterion TiO_2 NFs. (a) Wide-scan spectra. (b) N 1s spectra. (c) C 1s spectra. (d, e) TEM images of zwitterion TiO_2 NFs.

XFUF076, Millipore). A membrane area of 3.7 cm^2 was condensed to 0.2 MPa with distilled water for 40 min. To decrease the pressure at 0.1 MPa, the water flux of the membrane was determined as J_{w1} (L m^{-2} h). Subsequently, the 0.8 mg mL^{-1} BSA feed solution was displaced and relative fluxes were also measured at the same pressure. After 120 min of BSA filtration, the flux and concentration were evaluated using UV−vis spectroscopy (Schimadzu-1700) at 280 nm. The water flux of the cleaned membrane was denoted J_{w2} (L m^{-2} h). Antifouling was calculated as per the following equation

$$\text{FRR}\ (\%) = \left(\frac{J_{w2}}{J_{w1}}\right) \times 100 \tag{3}$$

where J_{w1} and J_{w2} are the BSA fluxes before and after each protein solution, respectively.

For the leaching test, membrane samples with dimensions of 2 × 2 cm^2 were sonicated in distilled water for 30 min. The leaching of TiO_2 nanoparticles into the solution was evaluated using inductively coupled plasma optical emission spectrometry (ICP-MS, Agilent, model 7500).[32]

2.8. Biocompatibility Studies. *2.8.1. Protein Adsorption.* Fluorescein isothiocyanate (FITC-BSA) (50 mg L^{-1}) was dissolved in phosphate-buffered saline (PBS) solution, and the solution was sealed with aluminum foil. The prepared membranes were cut into 3 × 3 cm^2 pieces, and each sample was rinsed in PBS. The prepared membrane samples were dipped in FITC-BSA PBS solution and kept in a dark room at 100 rpm for 10 h. Later, the membrane samples were gently rinsed with PBS solution to remove the loosely attached proteins, followed by immobilization of the proteins using glutaraldehyde. The amount of FITC-BSA adsorbed on the membrane samples was observed using fluorescence microscopy (Olympus BX61TRF).

2.8.2. Platelet Adhesion. The prepared membranes were evaluated for plate adhesion on their surfaces. In brief, the membrane samples were cut into 2 × 2 cm^2 sections after cleaning with PBS (pH 7.4) and placed in a 12-well plate. PRP

https://doi.org/10.1021/acsomega.1c02151
ACS Omega 2021, 6, 20279−20291

(200 μL) was dropped onto a specific membrane and preserved at 37 °C for 1 h. Later, the membranes were cleaned three times in PBS (pH 7.4), and the platelets observed on the membrane surface were stabilized with 1 wt % glutaraldehyde in PBS at 3 °C for 10 h. Lastly, the platelet-adhered membrane samples were rinsed with DI water and dried with serial concentrations of ethanol/water solutions (10, 30, 50, 70, 90, and 100 vol %). The membrane samples were examined for platelet morphological variations using FESEM analysis.

2.9. Cytotoxicity Studies. The cytotoxic effects of the prepared membranes were studied using peripheral blood mononuclear cells (PBMCs) obtained from human blood. The membrane samples (1 × 1 cm^2) were placed in 24-well plates with 200 μL of PBMCs and preserved at 37 °C for 4 h. The dead and live cells were classified using TO and PI dye. The cells were then suspended by adding 500 μL of PBS and evaluated by flow cytometry (BD FACScalibur).[33]

2.10. Antibacterial Activity. The antibacterial activities of the membranes were investigated using *Escherichia coli* and *Staphylococcus aureus* at initial concentrations of 10^6 CFU mL^{-1} using the zone inhibition method. The membranes were tested three times every 12 h to carry out the cycling inhibition measurements, and a camera was used to analyze the zone of inhibition. The killing ratios of bacteria in aqueous solutions were investigated by dipping 2 × 2 cm^2 membranes into bacterial suspensions. Bacterial culturing was performed for 12 h at 37 °C in a shaking incubator and observed for the inhibition zone.

3. RESULTS AND DISCUSSION

3.1. Characterization of Zwitterion TiO_2 NFs. Figure S1 shows the Fourier transform infrared (FTIR) spectra of TiO_2 and the zwitterion TiO_2. The TiO_2 spectrum shows adsorption peaks at 3400 and 1638 cm^{-1}, corresponding to the hydroxyl group (−OH) stretching vibrations. The wide peak at 500−600 cm^{-1} can be attributed to Ti−O−Ti-bond stretching vibrations. After modification of the TiO_2 NFs with lysine (amino acid), adsorption peaks appeared at 3085, 1620, and 1513 cm^{-1}, indicating the presence of $-NH_3^+$ and $-COOH^-$ groups. At high wavelengths between 2782 and 3085 cm^{-1}, the spectrum exhibits a N−H stretching adsorption band. The sharp peak at 1113 cm^{-1} is associated with C−O stretching vibrations. Moreover, the peaks at 1236, 1306, and 1361 cm^{-1} represent the stretching vibrations of the −OH and $-COO^-$ groups, corresponding to the carboxyl group of lysine. Hence, it was confirmed that lysine with $-NH_3^+$ and $-COOH^-$ groups was successfully grafted onto the TiO_2 surface. Figure 2a shows the XPS wide-scan spectrum of lysine surface grafting of TiO_2. The zwitterion TiO_2 was composed of four elements: Ti, C, O, and N. The N and C peaks corresponding to lysine confirmed the surface grafting of lysine onto TiO_2. The individual N 1s spectra shown in Figure 2b indicate high-resolution peaks corresponding to $-NH^{3+}$ group formation. The peaks at 400.2 and 400.8 eV correspond to $-NH^{3+}$ and $-NH^{2+}$, respectively, a dissociated form of lysine. Figure 2c shows the high resolution of the C 1s region with three different spectra. The binding energy of 288.8 eV is assigned to the carboxyl functional group (COO^-), whereas that of 286.7 eV indicates a tertiary carbon, which was connected to the amino functional group, and the lowest binding energy of 285.4 eV was assigned to the carbon methyl group. The intensities of the three peaks are in accordance with the C 1s spectra of lysine.[34,35] These $-NH^{3+}$ and $-COO^-$ groups were present on the surface of TiO_2 and exhibited a zwitterion charge. TEM images of the zwitterion TiO_2 NFs are displayed in Figure 2d,e. The TEM images show that the TiO_2 NFs had a 1D structure with an average diameter of 100−120 nm.

3.2. Membrane Characterization. *3.2.1. FTIR and Contact Angle Studies.* Figure S2 displays the FTIR analysis of the membranes. In comparison with the ZT-1 membrane sample, a slight hump at ∼1628 cm^{-1} is seen for the ZT-2, ZT-3, and ZT-4 membranes. This might be ascribed to the presence of a N−H bending vibration, confirming the presence of surface-grafted lysine in the zwitterion PES membranes. In comparison with the ZT-1 membrane, a new peak at 1306 cm^{-1} is seen for the ZT-2, ZT-3, and ZT-4 membranes. This peak represents stretching vibrations of $-COO^-$ groups corresponding to the carboxyl group of lysine. Hence, the zwitterion PES membranes exhibited the presence of functional groups, thereby establishing that the zwitterion property with hydrophilic surfaces would prevent both platelet adhesion and protein adsorption, which could provide a biointerface with promising antifouling properties.[36−38] Static contact angle analysis was performed to estimate the wettability of the membranes. The sessile drop method is the most versatile technique to evaluate the hydrophilicity of membranes, as shown in Figure S3. The hydrophilicity of the ZT-1 membrane was 75 ± 1°, which showed that the water had a low interaction on the membrane surface. The ZT-2, ZT-3, and ZT-4 membranes displayed enhanced hydrophilicity, with contact angles of 61 ± 3, 53 ± 2, and 50 ± 1°, respectively, corresponding to the zwitterion TiO_2 NF contents of 0.4, 0.6, and 1.2 wt %, respectively. The zwitterion membranes containing lysine on the TiO_2 NFs enhanced their hydrophilicity. Because the presence of both anionic and cationic groups can bind large amounts of free water, good hydrophilicity was evident. During the development of the zwitterion properties in the membranes, most of the hydrophilic zwitterion TiO_2 NFs were disposed to transfer toward the top layer to decrease the interfacial energy, thus decreasing the water contact angle.

3.2.2. Surface Topography and BET Analysis. The surface roughness parameters were studied using AFM. Figure 4d shows the three-dimensional (3D) images of the prepared membranes at a scan size of 5 × 5 μm^2. The membrane surface roughness was increased by the addition of zwitterion TiO_2, as illustrated in Table 1. The uniform dispersion of zwitterion TiO_2 in the PES matrix, as represented by a peak-and-valley-type morphology, was visualized as dark and bright regions, respectively. The average surface roughness values drastically increased from 73.85, 81.07, 90.40, and 146.82 nm for the ZT-1, ZT-2, ZT-3, and ZT-4 membranes, respectively. In the case of the ZT-2, ZT-3, and ZT-4 membranes, the zwitterion TiO_2 interacted with the amine and carboxylic groups, and therefore, increased surface roughness induced by hydrogen bonding was observed. As the loading increased from 0.4 to 1.2 wt% of zwitterion nanomaterial, the average surface roughness of the membrane increased significantly from 73.85 to 146.82 nm. This behavior can be explained by the interaction between the nanoparticles and the functional groups such as amine and carboxylic functional groups. The enhancement of surface roughness increases on the ZT-4 membrane could be due to the formation of zwitterion on TiO_2 nanoparticles through interfacial reaction. Therefore, increase in surface roughness due to induced hydrogen bonding has been observed in

https://doi.org/10.1021/acsomega.1c02151
ACS Omega 2021, 6, 20279−20291

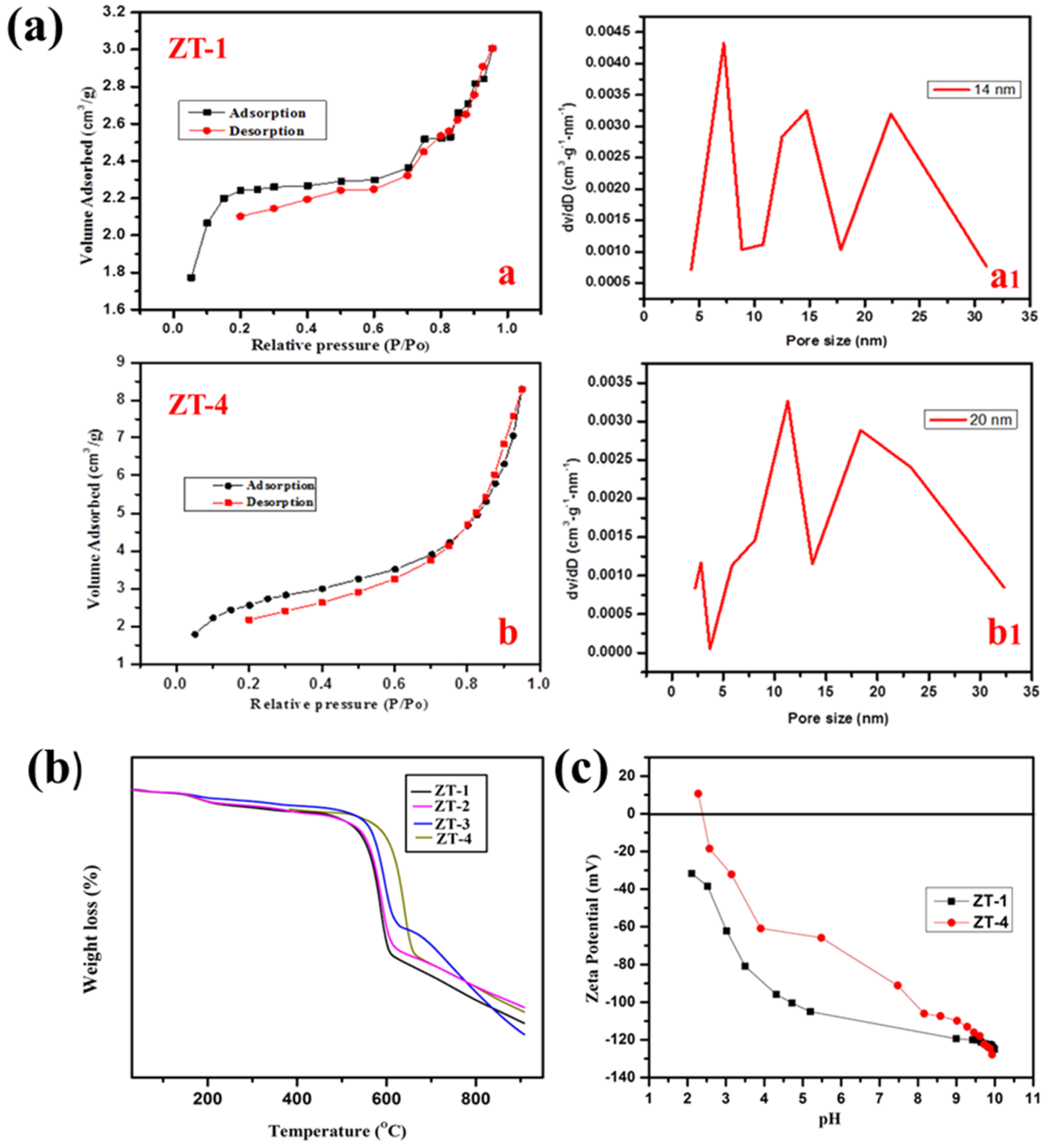

Figure 3. (a) Nitrogen adsorption and desorption isotherms and pore-size distribution of the (a, a_1) ZT-1 and (b, b_1) ZT-4 membranes. (b) Thermal stability and (c) ζ-potential analyses of membranes.

modified ZT-2, ZT-3, and ZT-4 membranes. N_2 adsorption and desorption studies were carried out to analyze the specific surface area, the Barrett−Joyner−Halenda (BJH) adsorption criteria, and the pore volumes of the pristine PES and zwitterion membranes. The nitrogen adsorption−desorption isotherms yielded an observable hysteresis loop that exemplified a mesoporous structure, and the corresponding pore-size distributions of the ZT-1 and ZT-4 membranes are shown in Figure 3a. The specific BET surface areas and pore-size distributions of the ZT-1 and ZT-4 membranes were 8.8756 and 7.4562 m^2 g^{-1} and 9.8628 and 7.0894 nm, respectively. Figure $3a_1$,b_1 represents the pore-size distribution of the PES and zwitterion-modified PES membranes, and the average pore size was in the range of 14−20 nm. With the addition of zwitterion TiO_2 in the PES matrix, the pore-size distribution gradually increased. An identical distribution of the mesoporous structure was clearly observed in the SEM images and should favor the permeability studies.

3.2.3. Thermogravimetric and ζ-Potential Analyses. Figure 3b shows the thermal behavior of the PES and zwitterion-modified PES membranes, and the decomposition values are shown in Table 1. When the PES membrane was investigated by thermogravimetric analysis from 30 to 900 °C, the membranes exhibited three major weight losses. The primary weight loss over 100 °C can be attributed to the evaporation of water and solvent. The secondary weight loss over 150−450 °C could be ascribed to the decomposition of amine and carboxylic groups. At the third weight loss stage, the

https://doi.org/10.1021/acsomega.1c02151
ACS Omega 2021, 6, 20279−20291

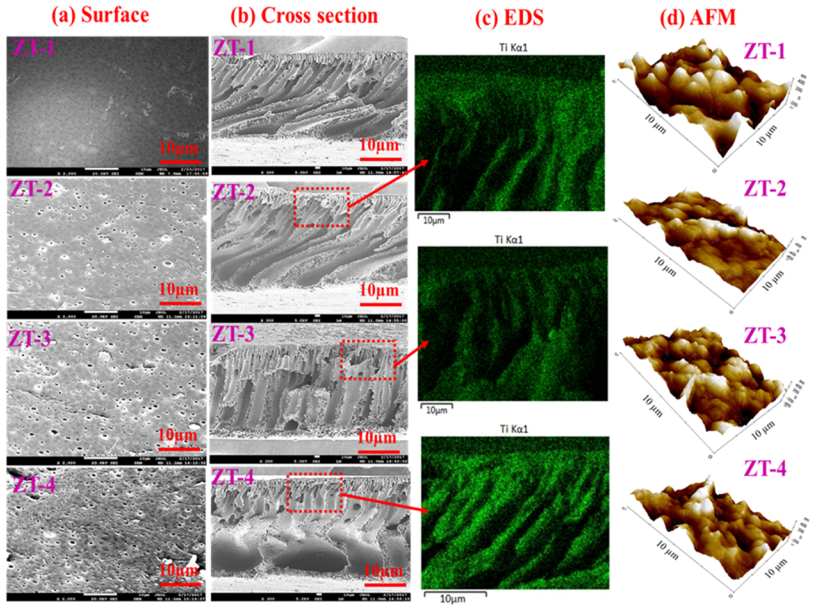

Figure 4. FESEM morphologies of membranes: (a) top surface, (b) cross section, (c) EDS mapping analysis, and (d) surface roughness of membranes.

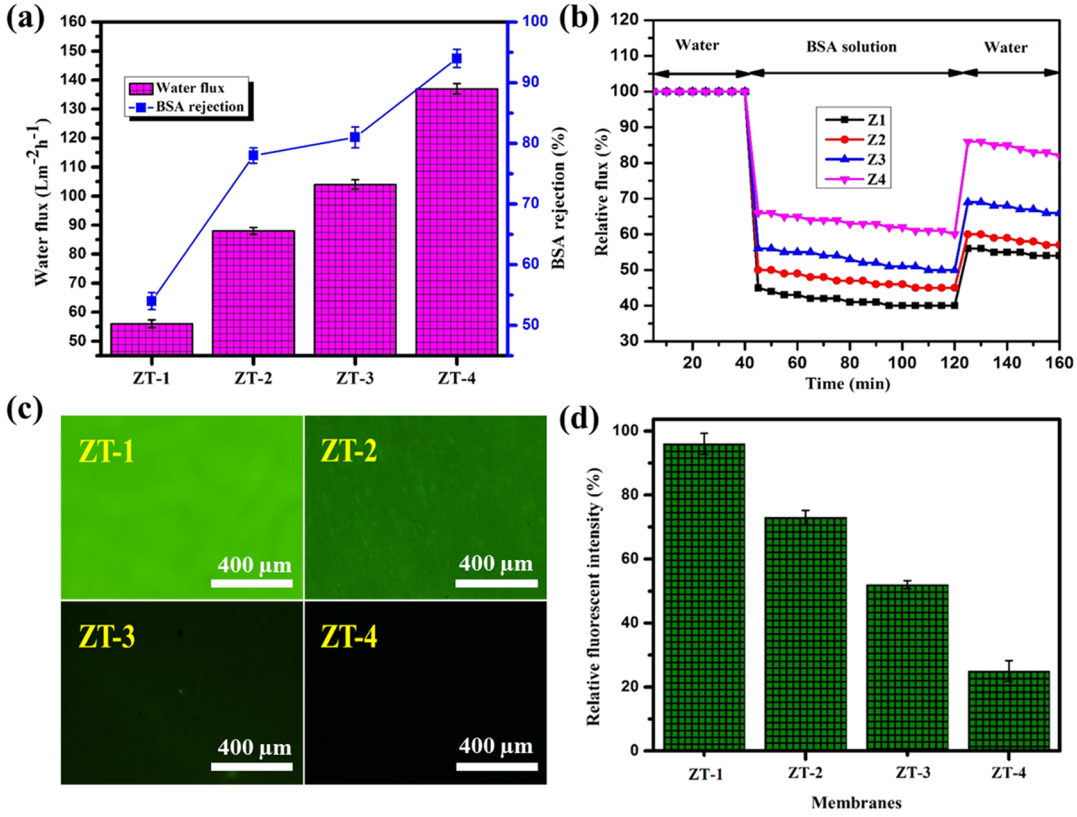

Figure 5. (a) Pure water flux and BSA rejection (b), relative flux, (c) fluorescence microscopy images of protein adsorption, and (d) intensity of fluorescence microscopy images.

increased thermal decomposition temperature for the ZT-2, ZT-3, and ZT-4 zwitterion membranes might be related to the incorporation of zwitterion TiO_2 into the PES membrane. Therefore, lysine and zwitterion TiO_2 delayed the degradation of the PES main polymer chains, leading to improved thermal stability. Surface charge is an essential criterion for evaluating the performance of the prepared pristine PES and zwitterion PES membranes. As shown in Figure 3c, the surface charge of the ZT-1 pristine PES membrane was mainly negative (−28 mV) in the pH range of 2−10. The increased surface charge density of the ZT-4 membrane was owing to the addition of zwitterion TiO_2 NFs in the range of pH 3−10 at 16 mV. A possible explanation for the increasing charge despite the electrically neutral lysine could be attributed to the formation

https://doi.org/10.1021/acsomega.1c02151
ACS Omega 2021, 6, 20279−20291

of zwitterion brushes owing to surface grafting onto TiO_2. These zwitterion brushes were available to cover the TiO_2 surface and led to the formation of a neutral charge density. The overall surface charge results of the zwitterion PES membranes were owing to the inclusive neutral charge densities that could be tuned by the addition of zwitterion TiO_2 in the PES matrix solution.

3.2.4. Membrane Morphology. The top-surface and cross-sectional morphologies of the PES and zwitterion-modified PES membrane morphologies were studied using FESEM, and the results are shown in Figure 4. The top surface of the ZT-1 membrane was smooth, with no pore formation or particles. However, the top surfaces of the ZT-2, ZT-3, and ZT-4 membranes showed gradual increases in pore size compared to that observed with the addition of zwitterion TiO_2. In addition, zwitterion TiO_2 produced no cracks on the top surfaces of the membranes, indicating that the membranes were not brittle in nature and were stable following the addition of zwitterion nanocomposite fillers. Figure 4a clearly reveals the distribution of nanocomposite fillers in the ZT-2, ZT-3, and ZT-4 membranes and the corresponding increases in membrane pore size. The cross-sectional FESEM images of the membranes are shown in Figure 4b; the membrane surfaces are smooth, which varied because of the different amounts of zwitterion TiO_2 loaded. Furthermore, no further agglomeration was observed owing to the addition of surface zwitterion TiO_2. On addition of TiO_2 nanofibers in the PES matrix, a significant difference in pore formation among ZT-2, ZT-3, and ZT-4 membranes was observed in the surface morphology of the membrane by FESEM analysis (Figure 4) as compared to the pristine ZT-1 membrane. This finding indicates that the lysine grafted on TiO_2 acted as a pore-forming additive in the preparation of the PES matrix and increased the pore structure on the membrane surface due to the presence of amine and carboxylic groups. In addition, the lysine grafted on TiO_2 can also act as a pore-forming additive in the preparation of PES membranes. The elemental distribution was analyzed using EDS, and the results are shown in Figure 4c. The EDS results revealed that zwitterion 1D TiO_2 NFs were present in the PES polymer matrix. The zwitterion 1D TiO_2 NF nanoparticles blended into the PES matrix, enhancing the membrane properties such as thermal stability, contact angle, antifouling, and biocompatibility and reduced the cytotoxicity.

3.3. Flux, Antifouling Studies, and Leaching Test. Zwitterion membranes are hydrophilic, which would generally affect protein adsorption on membranes, and are crucial to the antifouling property and protein filtration studies. Flux and BSA rejection analyses results for the prepared membranes are displayed in Figure 5a. The flux of the ZT-1 membrane was 56 ± 1.4 L m^{-2} h^{-1}. The zwitterion property and high porosity played an important role in increasing the water flux of the ZT-4 membrane, which was 137 ± 1.8 L m^{-2} h^{-1}. The ZT-4 membrane flux was thus 3 times higher than that of the ZT-1 membrane. As shown in Figure 5a, the PES membrane displayed a lower BSA rejection of up to 54 ± 2%. BSA rejection increased gradually up to 94 ± 1% for the ZT-4 membrane. It is interesting to note that the rejection increased with increasing loading of the zwitterion TiO_2 in the PES matrix. Moreover, the relative flux percentage was also higher for the ZT-4 membrane. Membrane pore size is one of the main factors for BSA rejection. The maximum BSA rejection was due to the following reasons. Firstly, the surface of the membrane is more hydrophilic due to the existence of the zwitterion lysine. The interactions with amine and carboxyl groups in lysine and water molecules form a thin hydration layer between the BSA foulants and the membrane surface.[39] This hydration layer increases the permeability of the membranes as well as obstructs the contact between BSA and the membrane surfaces. Second, BSA is negatively charged at pH 7.4,[40] while the zwitterion-modified membrane is also neutrally charged because of the existence of amine and carboxyl groups. Thus, electrostatic repulsion between neutrally charged membrane surfaces and BSA molecules also impeded the attachment of BSA to the membrane surface.[41] From Figure 5b, it can be seen that the rate of decrease of the final water flux was also minimal for the ZT-4 membrane owing to the zwitterion TiO_2 increasing the hydrophilic properties of the membrane surfaces. Zwitterion TiO_2 contained $-NH_3^+$ and $-COO^-$ groups on the surfaces, and thus, the zwitterion PES membranes were resistant to the adsorption of BSA molecules on their surfaces. Thus, the present study clearly shows that the surface functionality of the PES membrane improved with the addition of zwitterion TiO_2, which is a key requirement for hemocompatibility.

A comparison of different ultrafiltration membranes established for water flux and BSA protein rejection is summarized in Table 2. However, the newly synthesized zwitterion TiO_2 nanomaterial enabled a fouling-resistant zwitterion-modified PES membrane that not only generated water flux but also delivered better BSA protein rejection compared to some reported ultrafiltration membranes. Moreover, the protein rejection rate (94 ± 1%) and water flux (137 ± 1.8) values were higher than those of ultrafiltration membranes. For example, functionalization of polyacrylonitrile with tetrazole displayed a BSA rejection of 80.1% and a flux of 242.1 L m^{-2} h^{-1} bar^{-1}.[44] The higher removal of the zwitterion TiO_2 PES membranes should be ascribed to electrostatic repulsion between the membrane surface and BSA.

Table 2. Comparison of Pure Water Flux and Protein Rejection of Membranes in the Literature

membrane	pure water flux (L m^{-2} h^{-1})	protein rejection	ref
sulfonated polyaniline PVDF membrane	160	90% BSA	42
PVDF/Cu_xO/GO	206.45	80.73% BSA	43
TZ-PAN	242.1	80.1% BSA	44
PVDF/PVDF-g-PACMO	198	90% BSA	45
PVA/PAN	290	95% BSA	46
zwitterion TiO_2 PES	137 ± 1.8	94 ± 1% BSA	this work

Leaching tests were performed to measure the stability of the prepared TiO_2 PES membranes. The incorporated zwitterion TiO_2 amounts were 0.4, 0.6, and 1.2 wt % for ZT-2, ZT-3, and ZT-4, respectively. After 10 days, a small quantity of the zwitterion TiO_2 leached, leaving 99% of the PES polymer matrix (Figure 6). The results of this filtration experiment suggest that the antibacterial properties and antifouling properties of the zwitterion TiO_2 PES membrane can be stable over a long separation process.

3.4. BSA Adsorption. To examine the protein resistance of the zwitterion membranes, they were mixed in fluorescein-labeled BSA protein solution (BSA-FITC). Figure 5c shows the fluorescent images of the membranes. The ZT-1

https://doi.org/10.1021/acsomega.1c02151
ACS Omega 2021, 6, 20279−20291

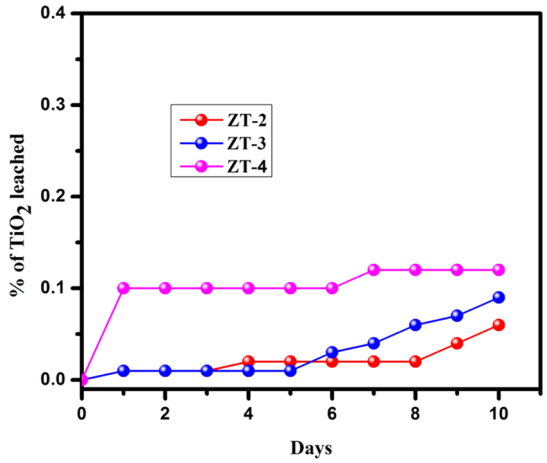

Figure 6. Leaching test for the prepared ZT-2, ZT-3, and ZT-4 membranes.

membrane shows a uniform and intense fluorescence, denoting that a significant volume of BSA proteins adsorbed onto the membrane surface because of the interactions between the benzene rings of PES and BSA. BSA adsorption gradually decreased with the addition of zwitterion TiO_2 to the PES membranes. The ZT-1 membrane showed a higher amount of BSA solution covering the surface of the membrane (Figure 5d), with a relative fluorescent intensity of ~92.2 ± 3%, whereas the modified ZT-2, ZT-3, and ZT-4 membranes showed decreased fluorescent intensities of 73.2 ± 4, 52.2 ± 1, and 25.8 ± 3%, respectively. It was confirmed that the hydrophilic zwitterion TiO_2 was extremely hydrated because of the zwitterion $-NH_3^+$ and $-COO^-$ functional groups developing a dense hydration layer. Thus, the hydration layers resisted protein adsorption on the zwitterion membrane surfaces. The nonpolar amino acid lysine, which was surface-grafted onto TiO_2 and incorporated into the PES membranes, exhibited excellent performance by suppressing the BSA protein owing to the formation of zwitterion membrane surfaces. It is well understood that zwitterion membranes form hydration layers via electrostatic interactions and hydrogen bonds. Hence, the membranes allowed a significant amount of water on their surfaces, which is a prominent repulsive force to the protein.[47,48] Otherwise, the enhanced protein adsorption resistance might be ascribed to the zwitterion structure formation.[49]

3.5. Platelet Adhesion. The adhesion of platelets to the membrane surface of biomaterials is another parameter for evaluating the hemocompatibility. When a foreign material comes into direct contact with the blood, adsorption of blood proteins, platelet adhesion, and platelet activation occur immediately, leading to thrombus formation.[50−52] Platelet adhesion assays are commonly used to evaluate the blood contact materials used in prepared membranes. Platelet adhesion on the membrane is categorized into five stages: discoid, dentric, spread/dentric, spreading, and fully spreading.[53,54] When an unsuitable material interacts with the blood, the platelets are inclined to spread through the membrane surfaces. Figure 7 shows the typical FESEM images of platelets adhered onto the membrane surface. For the PES (Z-1) membrane, the adhering platelets were flattened, and irregularly shaped pseudopodia were observed, indicating thrombus formation, which is a life-threatening phenomenon

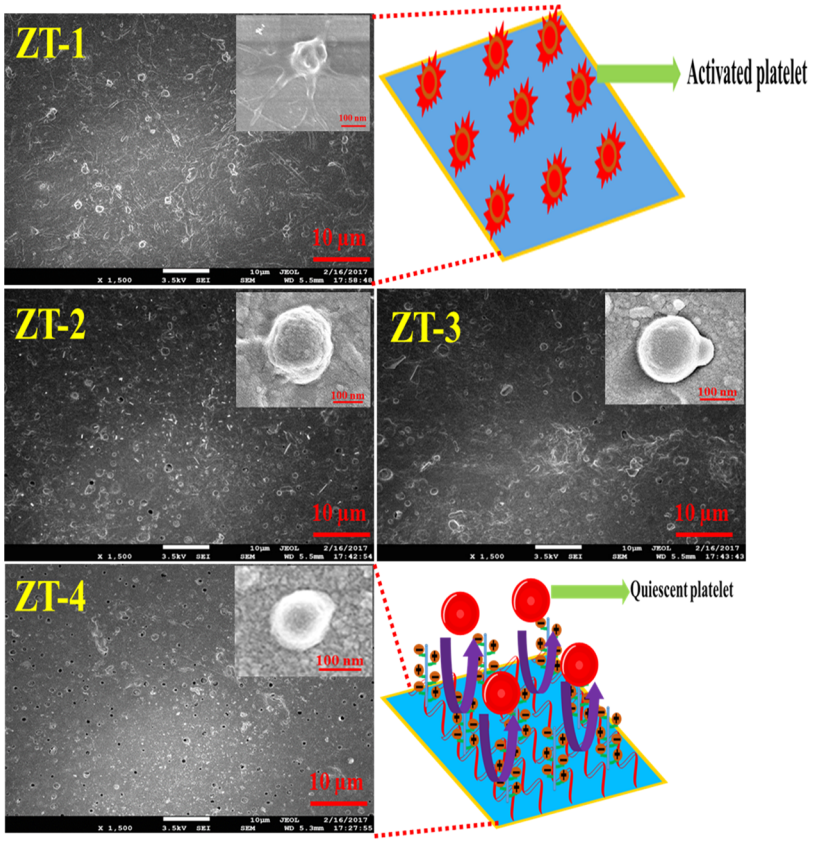

Figure 7. FESEM images of the surface platelets adhered onto membranes.

https://doi.org/10.1021/acsomega.1c02151
ACS Omega 2021, 6, 20279−20291

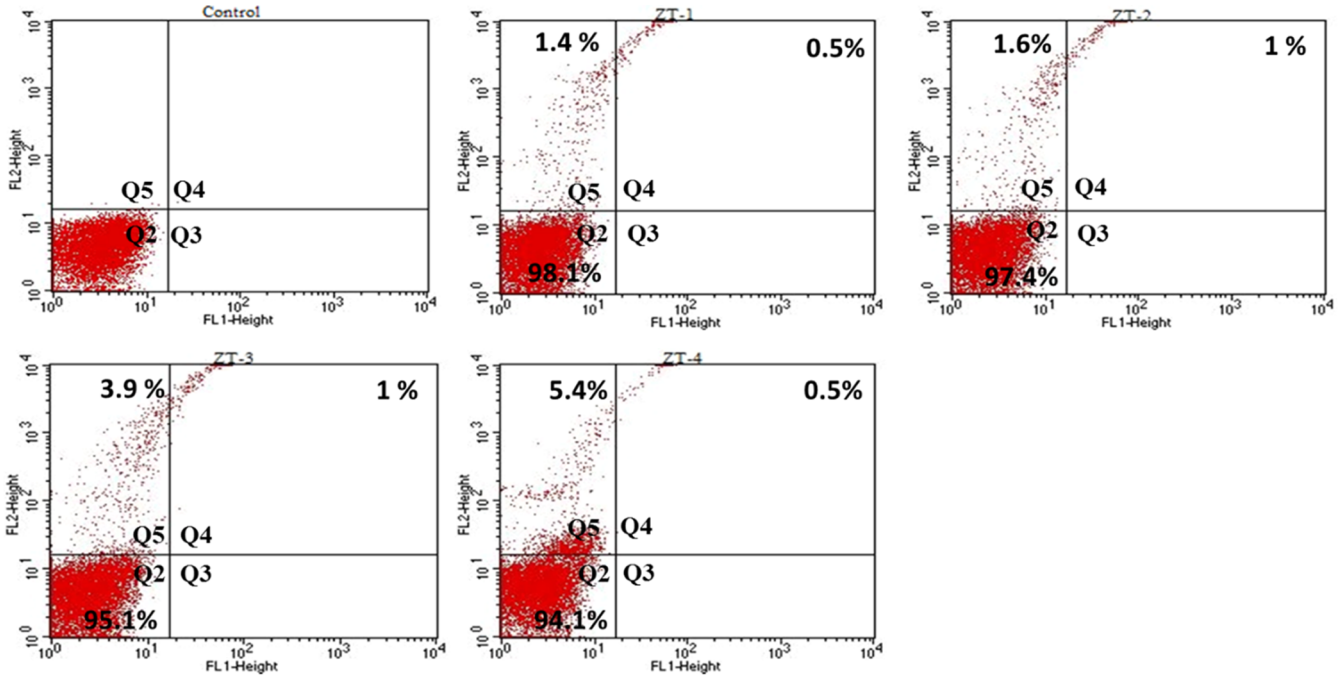

Figure 8. Flow cytometry analysis carried out in PBMCs for pristine PES and zwitterion PES membranes. Mean ± SD of three independent experiments, with each experiment conducted in triplicate.

in patients. After the addition of zwitterion TiO_2 into the PES Z-2, Z-3, and Z-4 membranes, the number of adherent platelets significantly decreased. These results show that the lysine-grafted TiO_2 exhibited zwitterion properties and effectively decreased the adherent platelets. It also maintained a rounded morphology, with no formation of pseudopodia or deformation, which was mainly affected by electrostatic interactions.

3.6. Cytotoxicity Studies. In biomedical applications, the intended tool should be used in nontoxic and pure forms. Flow cytometry analysis is an appropriate method to evaluate the percentage of live and dead cells. Figure 8 shows the flow cytometry analysis using PBMCs to study the cytotoxicity effects of the membranes. The prepared membranes were treated with PBMC, and after 4 h incubation, the membranes did not exhibit harmful effects on cell viability. The cell populations in different quadrants were analyzed using apoptosis analysis. The upper-right quadrant (Q5), upper-left quadrant (Q4), lower-right quadrant (Q3), and lower-left quadrant (Q2) indicate the dead cells, late apoptotic cells, early apoptotic cells, and live cells, respectively. Intercalating agents such as fluorescent PI and TO dyes were used as DNA stains to evaluate the cell viabilities of the dead and live cell representatives. To analyze the number of live and dead cells, PBMCs were treated with the pristine and modified membranes. For the ZT-1 membrane, 98.1% live cells were present as compared to the control cells. For the ZT-2-, ZT-3-, and ZT-4-modified zwitterion membranes with the addition of 1D TiO_2 NFs, 97.4, 95.1, and 94.1% live cells were present, respectively. Blood interaction with an external material normally results in thrombosis formation. Initially, the ZT-1 membrane was obviously not cytotoxic, consistent with the hydrophobic PES polymer and the low porous formation that increased cell entrapment, related to the earlier observation of increased compatibility between PBMCs. However, zwitterion modification of the ZT-2, ZT-3, and ZT-4 membranes led to drastic changes. In terms of platelet adhesion, SEM images of the modified membranes showed some platelets on the membrane surface. But PBMC cell adhesion was minimal, with a plateau corresponding to a 96.17% reduction in cell adhesion compared to the ZT-1 membrane. Both the modified and unmodified membranes had less toxicity against PBMCs after 4 h of incubation. Hence, the proposed zwitterion PES membranes could have promising biomedical applications.

3.7. Antibacterial Activity. For investigations of antibacterial activity, Gram-negative *E. coli* and Gram-positive *S. aureus* were preferred. Moreover, *E. coli* and *S. aureus* are the most common causes of bloodstream infections in humans owing to clinical treatment.[55] The pristine PES and zwitterion PES membranes were evaluated for their inhibitory activities against *E. coli* and *S. aureus*. Figure 9a,c shows that the ZT-1 membrane showed almost no zone inhibition ability. This is because the zwitterion nanomaterial is absent in the ZT-1 membrane. However, because of the addition of zwitterion 1D TiO_2 NFs, the ZT-4 membrane showed significant inhibition effects against *E. coli* and *S. aureus*, as clearly displayed in Figure 9b,d, respectively. The size of the inhibition zone against *E. coli* for the ZT-4 membrane was 4.8 ± 5 mm, and the size of the inhibition zone against *S. aureus* for the ZT-4 membrane was 2.6 ± 2 mm. The zwitterion ZT-4 membrane comprises both positively and negatively charged ($-NH_2^+$ and $-COOH^-$) groups, which was clearly confirmed in the membrane ζ-potential studies. Antimicrobial attachment on the membrane surface was prevented owing to the bacteriostatic effect (charge-based interactions). First, the NH_3^+ cations on the surface membrane repelled Gram-positive *S. aureus*. The positively charged membrane surface damaged *S. aureus* by affecting its metabolic functions. Second, the $-COOH^-$ anions on the membrane surface repelled Gram-negative *E. coli*, in which the negatively charged surface damaged the membrane surface of the bacteria, again by affecting their metabolic functions. These results clearly

https://doi.org/10.1021/acsomega.1c02151
ACS Omega 2021, 6, 20279−20291

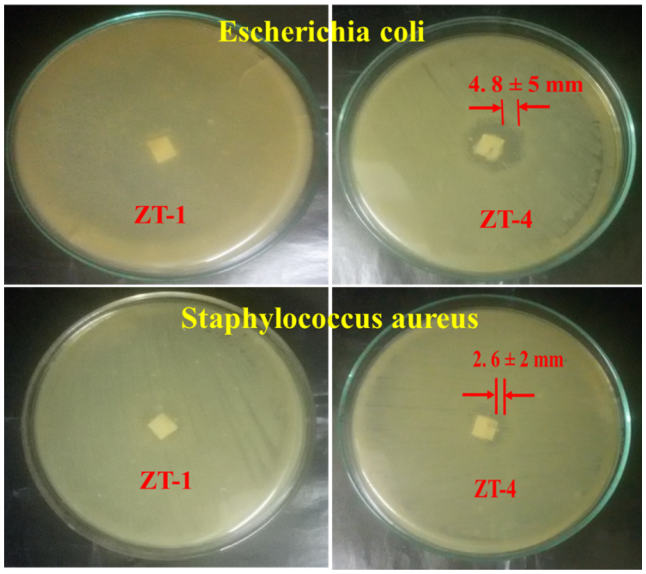

Figure 9. Antibacterial activities of ZT-1 and ZT-4 membranes.

demonstrated that the zwitterion TiO_2 PES membranes offered antimicrobial properties against *E. coli* and *S. aureus*.

4. CONCLUSIONS

In this study, the zwitterion TiO_2 nanomaterial incorporated in the PES matrix was successfully fabricated through the phase inversion method. The analysis results of ATR-FTIR and XPS confirmed that the zwitterion lysine had been successfully grafted on the TiO_2 nanomaterials. The zwitterion TiO_2 NFs were found to be uniformly distributed in the PES matrix, as observed in the SEM images. The contact angle, surface roughness, surface charge, and thermal stability of the zwitterion membranes all significantly increased by the addition of zwitterion TiO_2 NFs. Moreover, the antifouling properties and BSA rejection of zwitterion membranes improved significantly owing to the surfaces grafted with charged lysine amino acids having $-NH_3^+$ and $-COO$ functional groups. More importantly, as-prepared zwitterion brushes are demonstrated to have ultralow biofouling and extreme blood compatibility realized by systematic protein adsorption and platelet adhesion. Furthermore, the functional groups of the zwitterion brushes are tunable for the desired performance. This facile, versatile, and universal surface modification strategy is expected to be widely applicable in various advanced biomaterials and devices.

■ ASSOCIATED CONTENT

Supporting Information

The Supporting Information is available free of charge at https://pubs.acs.org/doi/10.1021/acsomega.1c02151.

FTIR spectra; FTIR analysis of the membrane; and water contact angle analysis of the membrane (PDF)

■ AUTHOR INFORMATION

Corresponding Author

G. Arthanareeswaran − *Membrane Research Laboratory, Department of Chemical Engineering, National Institute of Technology, Tiruchirappalli 620015, India;* orcid.org/0000-0001-9080-3592; Email: arthanaree10@yahoo.com

Authors

Kanagaraj Venkatesh − *Membrane Research Laboratory, Department of Chemical Engineering and Nanomaterials Laboratory, Department of Physics, National Institute of Technology, Tiruchirappalli 620015, India*

Palaniswamy Suresh Kumar − *Environmental & Water Technology Centre of Innovation (EWTCOI), Ngee Ann Polytechnic, 599489, Singapore*

Jihyang Kweon − *Water Treatment and Membrane Laboratory, Department of Environmental Engineering, Konkuk University, Seoul 05029, Republic of Korea*

Complete contact information is available at: https://pubs.acs.org/10.1021/acsomega.1c02151

Notes

The authors declare no competing financial interest.

■ ACKNOWLEDGMENTS

The work was partially supported by the National Research Foundation, South Korea, under the Brain Pool Program Grant No. 2019H1D3A2A01102322.

■ REFERENCES

(1) Rana, D.; Matsuura, T. Surface Modification for Antifouling Membranes. *Chem. Rev.* **2010**, *110*, 2448−2471.

(2) Zhao, C.; Xue, J.; Ran, F.; Sun, S. Modification of Polyethersulfone Membranes - A Review of Methods. *Prog. Mater. Sci.* **2013**, *58*, 76−150.

(3) Kuroki, H.; Tokarev, I.; Nykypanchuk, D.; Zhulina, E.; Minko, S. Stimuli-Responsive Materials: Stimuli-Responsive Materials with Self-Healing Antifouling Surface via 3D Polymer Grafting. *Adv. Funct. Mater.* **2013**, *23*, 4390.

(4) Xia, Y.; Cheng, C.; Wang, R.; Qin, H.; Zhang, Y.; Ma, L.; Tan, H.; Gu, Z.; Zhao, C. Surface-engineered nanogel assemblies with integrated blood compatibility, cell proliferation and antibacterial property: towards multifunctional biomedical membranes. *Polym. Chem.* **2014**, *5*, 5906−5919.

(5) Kwak, S. Y.; Kim, S. H.; Kim, S. S. Hybrid organic/inorganic reverse osmosis (RO) membrane for bactericidal anti-fouling. 1. Preparation and characterization of TiO_2 nanoparticle self-assembled aromatic polyamide thin-film-composite (TFC) membrane. *Environ. Sci. Technol.* **2001**, *35*, 2388−2394.

(6) Lee, S. H.; Gupta, M. K.; Bang, J.; Bae, B. H.; Sung, H. J. Current Progress in Reactive Oxygen Species (ROS)-Responsive Materials for Biomedical Applications. *Adv. Healthcare Mater.* **2013**, *2*, 908−915.

(7) Zhao, Y. F.; Zhu, L. P.; Yi, Z.; Zhu, B. K.; Xu, Y. Y. Improving the hydrophilicity and fouling-resistance of polysulfone ultrafiltration membranes via surface zwitterionicalization mediated by polysulfone-based triblock copolymer additive. *J. Membr. Sci.* **2013**, *440*, 40−47.

(8) Zhu, L.; Liu, F.; Yu, X.; Xue, L. Poly(Lactic Acid) Hemodialysis Membranes with Poly(Lactic Acid)-block-Poly(2-Hydroxyethyl Methacrylate) Copolymer As Additive: Preparation, Characterization, and Performance. *ACS Appl. Mater. Interfaces* **2015**, *7*, 17748−17755.

(9) Chang, T.; DeFine, L.; Alexander, T.; Kyu, T. In vitro investigation of antioxidant, anti-Inflammatory, and antiplatelet adhesion properties of genistein-modified poly(ethersulfone)/poly-(vinylpyrrolidone) hemodialysis membranes. *J. Biomed. Mater. Res., Part B* **2015**, *103*, 539−547.

(10) Irfan, M.; Idris, A.; Yusof, N. M.; Khairuddin, N. F. M.; Akhmal, H. Surface modification and performance enhancement of nano-hybrid f-MWCNT/PVP90/PES hemodialysis membranes. *J. Membr. Sci.* **2014**, *467*, 73−84.

(11) Tripathi, B. P.; Dubey, N. C.; Stamm, M. Polyethylene glycol cross-linked sulfonated polyethersulfone based filtration membranes with improved antifouling tendency. *J. Membr. Sci.* **2014**, *453*, 263−274.

(12) Fu, W.; Carbrello, C.; Wu, X.; Zhang, W. Visualizing and Quantifying the Nanoscale Hydrophobicity and Chemical Distribution of Surface Modified Polyethersulfone (PES) Membranes. *Nanoscale* **2017**, *9*, 15550−15557.
(13) Banerjee, I.; Pangule, R. C.; Kane, R. S. Antifouling coatings: recent developments in the design of surfaces that prevent fouling by proteins, bacteria, and marine organisms. *Adv. Mater.* **2011**, *23*, 690−718.
(14) Tsai, M. Y.; Chen, Y. C.; Lin, T. J.; Hsu, Y. C.; Lin, C. Y.; Yuan, R. H.; Yu, J.; Teng, M. S.; Hirtz, M.; Chen, M. H. C.; et al. Antifouling: Vapor-Based Multicomponent Coatings for Antifouling and Biofunctional Synergic Modifications. *Adv. Funct. Mater.* **2014**, *24*, 2280.
(15) Yang, C.; Ding, X.; Ono, R. J.; Lee, H.; Hsu, L. Y.; Tong, Y. W.; Hedrick, J.; Yang, Y. Y. Brush-like polycarbonates containing dopamine, cations, and PEG providing a broad spectrum, antibacterial, and antifouling surface via one-step coating. *Adv. Mater.* **2014**, *26*, 7346−7351.
(16) Roberts, M. J.; Bentley, M. D.; Harris, J. M. Chemistry for peptide and protein PEGylation. *Adv. Drug Delivery Rev.* **2012**, *64*, 116−127.
(17) Harris, J. M.; Chess, R. B. Effect of pegylation on pharmaceuticals. *Nat. Rev. Drug Discovery* **2003**, *2*, 214−221.
(18) Pasut, G.; Veronese, F. M. Polymer-drug conjugation, recent achievements and general strategies. *Prog. Polym. Sci.* **2007**, *32*, 933−961.
(19) Canalle, L. A.; Lowik, D. W. P. M.; van Hest, J. C. M. Polypeptide−polymer bioconjugates. *Chem. Soc. Rev.* **2010**, *39*, 329−353.
(20) Veronese, F. M.; Pasut, G. PEGylation, successful approach to drug delivery. *Drug Discovery Today* **2005**, *10*, 1451−1458.
(21) Gombotz, W. R.; Guanghui, W.; Horbett, T. A.; Hoffman, A. S. Protein adsorption to poly(ethylene oxide) surfaces. *J. Biomed. Mater. Res.* **1991**, *25*, 1547−1562.
(22) Sofia, S. J.; Premnath, V.; Merrill, E. W. Poly(ethylene oxide) Grafted to Silicon Surfaces: Grafting Density and Protein Adsorption. *Macromolecules* **1998**, *31*, 5059−5070.
(23) McPherson, T. B.; Shim, H. S.; Park, K. Grafting of PEO to glass, nitinol, and pyrolytic carbon surfaces by gamma irradiation. *J. Biomed. Mater. Res.* **1997**, *38*, 289−302.
(24) Yuan, Y. L.; Zhang, J.; Ai, F.; Yuan, J.; Zhou, J.; Shen, J.; Lin, S. C. Surface modification of SPEU films by ozone induced graft copolymerization to improve hemocompatibility. *Colloids Surf., B* **2003**, *29*, 247−256.
(25) He, G.; Cai, Y.; Zhao, Y.; Wang, X.; Lai, C.; Xi, M.; Zhu, Z.; Fong, H. Electrospun anatase phase TiO_2 nanofibers with different morphological structures and specific surface areas. *J. Colloid Interface Sci.* **2013**, *398*, 103−111.
(26) Venkatesh, K.; Arthanareeswaran, G.; Chandra Bose, A.; Suresh Kumar, P. Hydrophilic hierarchical carbon with TiO2 nanofiber membrane for high separation efficiency of dye and oil-water emulsion. *Sep. Purif. Technol.* **2020**, *241*, No. 116709.
(27) Wang, J.; Wang, T.; Li, L.; Wu, P.; Pan, K.; Cao, B. Functionalization of polyacrylonitrile nanofiber using ATRP method for boric acid removal from aqueous solution. *J. Water Process Eng.* **2014**, *3*, 98−104.
(28) Rosen, J. E.; Gu, F. X. Surface functionalization of silica nanoparticles with cysteine: A low-fouling zwitterionic surface. *Langmuir* **2011**, *27*, 10507−10513.
(29) Chen, S.; Cao, Z.; Jiang, S. Ultra-low fouling peptide surfaces derived from natural amino acids. *Biomaterials* **2009**, *30*, 5892−5896.
(30) Cui, J.; Ju, Y.; Liang, K.; et al. Nanoscale engineering of low-fouling surfaces through polydopamine immobilisation of zwitterionic peptides. *Soft Matter* **2014**, *10*, 2656−2663.
(31) Nowinski, A. K.; Sun, F.; White, A. D.; Keefe, A. J.; Jiang, S. Sequence, structure, and function of peptide self-assembled monolayers. *J. Am. Chem. Soc.* **2012**, *134*, 6000−6005.
(32) Jiang, H.; Xu, F. J. Biomolecule-functionalized polymer brushes. *Chem. Soc. Rev.* **2013**, *42*, 3394−3426.
(33) Neelakandan, C.; Chang, T.; Alexander, T.; Define, L.; Evancho-Chapman, M.; Kyu, T. In vitro evaluation of antioxidant and anti-inflammatory properties of genistein-modified hemodialysis membranes. *Biomacromolecules* **2011**, *12*, 2447−2455.
(34) Shi, Q.; Su, Y. L.; Chen, W. J.; Peng, J. M.; Nie, L. Y.; Zhang, L.; Jiang, Z. Y. Grafting short-chain amino acids onto membrane surfaces to resist protein fouling. *J. Membr. Sci.* **2011**, *366*, 398−404.
(35) Xu, C.; Liu, X.; Xie, B.; Yao, C.; Hu, W.; Li, Y.; Li, X. Preparation of PES ultrafiltration membranes with natural amino acids based zwitterionic antifouling surfaces. *Appl. Surf. Sci.* **2016**, *385*, 130−138.
(36) Huang, J.; Xue, J.; Xiang, K.; Zhang, X.; Cheng, C.; Sun, S.; Zhao, C. Surface modification of polyethersulfone membranes by blending triblock copolymers of methoxyl poly(ethylene glycol) polyurethane methoxyl poly(ethylene glycol). *Colloids Surf., B.* **2011**, *88*, 315−324.
(37) Li, X.; Wang, M.; Wang, L.; Shi, X.; Xu, Y.; Song, B.; Chen, H. Block copolymer modified surfaces for conjugation of biomacromolecules with control of quantity and activity. *Langmuir* **2013**, *29*, 1122−1128.
(38) Liu, X.; Xu, Y.; Wu, Z.; Chen, H. Poly (N-vinylpyrrolidone)-modified surfaces for biomedical applications. *Macromol. Biosci.* **2013**, *13*, 147−154.
(39) Liu, Z.; Mi, Z.; Chen, C.; Zhou, H.; Zhao, X.; Wang, D. Preparation of hydrophilic and antifouling polysulfone ultrafiltration membrane derived from phenolphthalin by copolymerization method. *Appl. Surf. Sci.* **2017**, *401*, 69−78.
(40) Fakhfakh, S.; Baklouti, S.; Baklouti, S.; Bouaziz, J. Preparation, characterization and application in BSA solution of silica ceramic membranes. *Desalination* **2010**, *262*, 188−195.
(41) Wu, X.; Xie, Z.; Wang, H.; Zhao, C.; Ng, D.; Zhang, K. Improved filtration performance and antifouling properties of polyethersulfone ultrafiltration membranes by blending with carboxylic acid functionalized polysulfone. *RSC Adv.* **2018**, *8*, 7774.
(42) Qin, A.; Li, X.; Zhao, X.; Liu, D.; He, C. Engineering a Highly Hydrophilic PVDF Membrane via Binding TiO_2 Nanoparticles and a PVA Layer onto a Membrane Surface. *ACS Appl. Mater. Interfaces* **2015**, *7*, 8427−8436.
(43) Zhao, C.; Lv, J.; Xu, X.; Zhang, G.; Yang, Y.; Yang, F. Highly antifouling and antibacterial performance of poly (vinylidene fluoride) ultrafiltration membranes blending with copper oxide and graphene oxide nanofillers for effective wastewater treatment. *J. Colloid Interface Sci.* **2017**, *505*, 341−351.
(44) Zhao, W.; Liu, L.; Wang, L.; Li, N. Functionalization of polyacrylonitrile with tetrazole groups for ultrafiltration membranes. *RSC Adv.* **2016**, *6*, 72133−72140.
(45) An, Z.; Xu, R.; Dai, F. Y.; Xue, G. J.; He, X. L.; Zhao, Y. P.; Chen, L. PVDF/PVDF-g-PACMO blend hollow fiber membranes for hemodialysis: preparation, characterization, and performance. *RSC Adv.* **2017**, *7*, 26593−26600.
(46) Yu, X. F.; Shen, L. D.; Zhu, Y. D.; Li, X.; Yang, Y.; Wang, X. F.; Zhu, M. F.; Hsiao, B. S. High performance thin-film nanofibrous composite hemodialysismembranes with efficient middle-molecule uremic toxin removal. *J. Membr. Sci.* **2017**, *523*, 173−184.
(47) Zhang, Z.; Chen, S.; Chang, Y.; Jiang, S. Surface Grafted Sulfobetaine Polymers via Atom Transfer Radical Polymerization as Superlow Fouling Coatings. *J. Phys. Chem. B.* **2006**, *110*, 10799−10804.
(48) Ishihara, K.; Nomura, H.; Mihara, T.; Kurita, K.; Iwasaki, Y.; Nakabayashi, N. Why do phospholipid polymers reduce protein adsorption? *J. Biomed. Mater. Res.* **1998**, *39*, 323−330.
(49) Zhang, J.; Yuan, J.; Yuan, Y. L.; Zang, X. P.; Shen, J.; Lin, S. C. Platelet adhesive resistance of segmented polyurethane film surface-grafted with vinyl benzyl sulfo monomer of ammonium zwitterions. *Biomaterials* **2003**, *24*, 4223−4231.
(50) Wang, J.; Qiu, M.; He, C. A. Zwitterionic Polymer/PES Membrane for Enhanced Antifouling Performance and Promoting Hemocompatibility. *J. Membr. Sci.* **2020**, *606*, No. 118119.

https://doi.org/10.1021/acsomega.1c02151
ACS Omega 2021, 6, 20279−20291

(51) Li, C.; Zhang, M.; Liu, X.; Zhao, W.; Zhao, C. Immobilization of heparin-mimetic biomacromolecules on Fe_3O_4 nanoparticles as magnetic anticoagulant via mussel-inspired coating. *Mater. Sci. Eng. C* **2020**, *109*, No. 110516.
(52) Grunkemeier, J. M.; Tsai, W. B.; McFarland, M. C.; Horbett, T. A. The effect of adsorbed fibrinogen, fibronectin, von Willebrand factor and vitronectin on the procoagulant state of adherent platelets. *Biomaterials* **2000**, *21*, 2243−2252.
(53) Grunkemeier, J. M.; Tsai, W. B.; Horbett, T. A. Co-adsorbed fibrinogen and von Willebrand factor augment platelet procoagulant activity and spreading. *J. Biomater. Sci., Polym. Ed.* **2001**, *12*, 1−20.
(54) Li, J.; Huang, X. J.; Ji, J.; Lan, P.; Vienken, J.; Groth, T.; Xu, Z. K. Covalent Heparin Modification of a Polysulfone Flat Sheet Membrane for Selective Removal of Low-Density Lipoproteins: A Simple and Versatile Method. *Macromol. Biosci.* **2011**, *11*, 1218−1226.
(55) Haghighat, N.; Vatanpour, V.; Sheydaei, M.; Nikjavan, Z. Preparation of a Novel Polyvinyl Chloride (PVC) Ultrafiltration Membrane Modified with Ag/TiO_2 Nanoparticle with Enhanced Hydrophilicity and Antibacterial Activities. *Sep. Purif. Technol.* **2020**, *237*, No. 116374.

https://doi.org/10.1021/acsomega.1c02151
ACS Omega 2021, 6, 20279−20291